Clim. Past Discuss., 7, 521–534, 2011
www.clim-past-discuss.net/7/521/2011/
doi:10.5194/cpd-7-521-2011

Climate of the Past Discussions

Impact of North Atlantic – GIN Sea exchange on deglaciation evolution of Atlantic Meridional Overturning Circulation

J. Cheng[1], Z. Liu[2,3], F. He[2], and B. L. Otto-Bliesner[4]

[1]Key Laboratory of Meteorological Disaster of Ministry of Education and College of Atmospheric Sciences, Nanjing Univ. of Information Science and Technology, Nanjing, 210044, China
[2]Center for Climatic Research and Dept. Atmospheric and Oceanic Sciences, Univ. of Wisconsin-Madison, Madison, WI 53706, USA
[3]Laboratory for Climate and Ocean-Atmosphere Studies, Dept. of Atmospheric and Oceanic Sciences, School of Physics, Peking University, 100871, Beijing, China
[4]Climate and Global Dynamics Division, National Center for Atmospheric Research, Boulder, CO 80307-3000, USA

Received: 31 January 2011 – Accepted: 1 February 2011 – Published: 9 February 2011

Correspondence to: J. Cheng (chengjun@nuist.edu.cn)

Published by Copernicus Publications on behalf of the European Geosciences Union.

Abstract

The Bølling-Allerød (BA) warming is the most pronounced abrupt climate change event during the last deglaciation. Two notable features of the BA onset are found in our transient simulation of the last deglaciation with CCSM3: the first is the occurrence of an overshoot in the Atlantic Meridional Overturning Circulation (AMOC, about 20 Sv as to 13 Sv at Last Glacial Maximum) and the second is the subsequent transition of AMOC from a glacial (about 13 Sv) to an interglacial mean state (about 18 Sv). Here, we present two new sensitivity experiments to explicitly illustrate the impact of North Atlantic – GIN Sea exchange on the deglaciation evolution of the AMOC. In these sensitivity experiments, the oceanic exchange during the BA onset is inhibited by introducing a Partial Blocking scheme. In response to this, the deep-water formation in the GIN Sea is reduced by 80% compared to the transient simulation. This in turn results in a reduced AMOC overshoot followed by a lower mean state of the AMOC. Our results therefore suggest that, oceanic processes were more important than the external forcings and atmospheric processes for the AMOC evolution during the BA onset.

1 Introduction

The Bølling-Allerød event (BA, 14.6 kyr BP [ka]) was the most pronounced abrupt climate change event within the last deglaciation. An overshoot in the AMOC was recently suggested as a cause for the BA event (Liu et al., 2009). The overshoot phenomenon of the AMOC is a transient process that occurs after the cessation of the meltwater discharge in the North Atlantic (NA). Central to the process is an increase in the magnitude of AMOC strength change, which subsequently induces more intense climate change. Evidence of an AMOC overshoot during the BA event is provided by several marine proxy records at different locations and with different reconstruction basis (Stanford et al., 2006; Barker et al., 2009, 2010). Numerous model simulations, with different physical frameworks and complexity, suggest that the AMOC overshoot is a common and robust phenomenon in freshwater-hosing experiments (Manabe et al., 1997; Weaver et al., 2003; Knutti et al., 2004; Stouffer et al., 2006; Mignot et al., 2007; Weber et al., 2007; Krebs et al., 2007; Schmittner et al., 2008; Arzel et al., 2008).

In the first synchronously transient simulation of the last deglaciation with a fully-coupled climate model (TraCE-21000), an AMOC overshoot (about 20 Sv as to 13 Sv at Last Glacial Maximum, LGM) is simulated and shown to be a key contributor to the onset of BA warming (Liu et al., 2009). In TraCE-21000, surface air temperature (SAT) over Greenland increases about 10 °C during BA onset. The AMOC overshoot contributes about 6 °C warming of SAT over Greenland during the BA onset, while the other 4 °C warming is derived from the recovery of the AMOC strength from the collapsed state to the LGM level. Also, the spatial scale of the AMOC overshoot climatic effect is hemispherical (Liu et al., 2009). In TraCE-21000, the stable AMOC strength during BA is about 18 Sv, which is comparable with the values found in the interglacial simulations with the same model (CCSM) (Yeager et al., 2006). The main result of the AMOC overshoot during BA is the transition of the AMOC from a glacial to an interglacial mean state. Meanwhile, reconstructed SAT over Greenland during the last deglaciation show that the maximum SAT at BA is close to that under the current interglacial state (Cuffey and Clow, 1997), providing support for a mean state transition.

The importance of NA – GIN Sea exchange for the deep-water formation in Labrador and GIN Sea has been highlighted in several studies of Holocene climate evolution (de Vernal and Hillaire-Marcel, 2006; Hillaire-Marcel et al., 2007) and global warming (Hu et al., 2004). In many literatures about the recovery of a collapsed AMOC, oceanic advective processes are dominant (Vellinga et al., 2002; Krebs et al., 2007). As one part of these advective processes, the importance of NA – GIN Sea exchange for the AMOC recovery is still not explicitly discussed and tested, especially for its impact on the last deglaciation evolution of the AMOC. Here, we present results from additional sensitivity experiments to TraCE-21000, where we explicitly assess the impact of NA – GIN Sea exchange on the last deglaciation evolution of the AMOC and the deep-water formation in the Labrador and GIN Sea.

2 Model and experiment setup

The climate model used in this study is the low-resolution version of Community Climate System Model, Version 3 (CCSM3 T31_gx3v5) with a dynamic global vegetation module. CCSM3 is a global, coupled ocean-atmosphere-sea ice-land surface climate model without flux adjustment (Yeager et al., 2003; Collins et al., 2006). The atmospheric model is the CAM3 with horizontal resolution of about $3.75^\circ \times 3.75^\circ$ and 26 vertical hybrid coordinate levels. The land model is the CLM3 with same resolution as the atmosphere. The ocean model is the NCAR implementation of POP with vertical z-coordinate and 25 levels. The longitudinal resolution is 3.6 degree and the latitudinal resolution is variable, with finer resolution in the tropics and north Atlantic. The sea ice model is the CSIM with same resolution as the ocean model.

In this study, two sensitivity experiments are initiated from and compared to the DGL-A run of TraCE-21000. The forcing includes transient variations in the orbital parameters, the greenhouse gas (GHG, including CO_2, CH_4 and N_2O) concentrations (Joos and spahni, 2008), the continental ice sheets (Peltier, 2004) and the meltwater input (Liu et al., 2009). In addition, fixed coastlines under LGM state (Peltier, 2004) have been used. The DGL-A run starts from 22 ka and successfully reproduces several major features of the last deglaciation evolution (Liu et al., 2009).

The settings of the two sensitivity experiments are almost the same as for the DGL-A run except for employing a "Partially Blocking" (PB) scheme at the edge of the NA and GIN Sea during BA (see Supplement). The PB scheme is developed and used to diagnose the oceanic feedbacks (Liu et al., 2002; Wu and Liu 2002, 2003; Zhong et al., 2008) and involves prescribing a thin "sponge wall" of salinity and temperature in the ocean. In the PB zone, salinity and temperature of each grid cell are restored to the prescribed annual cycle of the specific condition (see below), other variables in this region are adjusted allodiality during the model integration. The restoring applies for depths below 50 m to avoid any influence of the PB scheme on the local air-sea interaction. As a consequence of this, the exchanges of heat and salt, as well as the wave propagation, through the PB zone are all inhibited.

CPD
7, 521–534, 2011

The first sensitivity experiment, named as PB_PreBA, restarts from 14.77 ka (the collapsed state of AMOC before BA). In the PB_PreBA run, the salinity and temperature of the PB zone are restored to the PreBA state (14.67 ka, start time of the BA onset in Liu et al., 2009). The initial 100 years integration of the PB_PreBA run (14.77–14.67 ka) shows that PB scheme doesn't induce significant shift of the AMOC strength (Fig. 1a). Similarly, the second sensitivity experiment, named as PB_REC, restarts from 14.5 ka (REC is the time when the AMOC strength is recovering to the LGM level and the overshoot is initiated). In the PB_REC run, the salinity and temperature of PB zone are restored to the REC state. For both sensitivity experiments, the restoring time scale is 90 days. Unlike the PB_PreBA run, the restart state of the PB_REC run is a transient one. The integration length of the PB_PreBA and the PB_REC run are 600 and 300 years, respectively.

3 Results

When implementing the PB scheme during the BA onset, the reinitiation of deep-water formation in the GIN Sea is reduced by nearly 100% and 80% for the PB_PreBA and the PB_REC run compared to the DGL-A run, respectively (red dash and solid line in Fig. 1a and b). The deep-water formation in the Labrador Sea is also affected, especially for the PB_PreBA run, where there is a reduction of about 2 Sv in its maximum value (blue solid and dash line in Fig. 1a and b).

The AMOC strength is based on the total amount of the deep-water formed in the Labrador and GIN Sea. In the PB_PreBA run, the lack of recovery of the deep-water formation in the GIN Sea prevents the AMOC from recovering to the glacial state, and leads to an overall weakening of about 3 Sv (black solid line in Fig. 1a). The restart state of the PB_REC run is transient, presenting as that the AMOC strength equals to the LGM level, but the deep-water formation amount in the Labrador Sea is enhanced and that in the GIN Sea is suppressed (Fig. 1b). The AMOC strength of the PB_REC run continuously stay around this level with opposite and near equally change of the deep-water formation amount in the Labrador and GIN Sea. The continuous changes of deep-water formation in the Labrador and GIN Sea in the PB_REC run are partially the results of its transient restart state. Compared to the DGL-A run, the total increase in the magnitude of the AMOC strength during the BA onset is reduced by about 11 Sv and 7 Sv in the PB_PreBA and the PB_REC run, respectively. As the results of this, the AMOC overshoot and the subsequent mean state transition are suppressed in both experiments.

The "sponge wall" of salinity and temperature at the edge of the NA and GIN Sea inhibits the salt and heat transport to the GIN Sea within the oceanic upper layers. Compared to the DGL-A run, the recovery ratios are about 27% and 60% for the northward salt transport, and 0% and about 11% for the northward heat transport in the PB_PreBA and the PB_REC run, respectively (Fig. 2a and b). Because the heat transport to the GIN Sea is inhibited, the sea ice concentration over the GIN Sea remains extensive. The meltback is only about 20% in the PB_REC run while there is no meltback of sea ice in the PB_PreBA run (Fig. 2c). The local oceanic heat loss (SHF) is mainly controlled by the extended sea ice concentration. The SHF remains near pre-recovery values and only increases about 23% in the PB_REC run and not at all in the PB_PreBA run (Fig. 2d). As the surface density flux is mainly dominated by the thermal part (Shin et al., 2003), the suppressed oceanic heat loss also results in a suppressed surface density flux. The surface density flux is known to dominate the "local" deep-water formation at high northern latitudes. Thus, the resumption of the local part of the deep-water formation during the BA onset is inhibited heavily.

The salt/dense water input within the upper layers to the GIN Sea during the BA onset is another "non-local" contributor to the reinitiation of the deep-water formation in the GIN Sea. This non-local factor only operates during the recovery process of the AMOC when the NA is freshened by meltwater discharge. Salt input within the upper layers to the GIN Sea is slightly resumed but not much (Fig. 2a), so the resumption of the non-local part of the deep-water formation in the GIN Sea is inhibited too.

CPD
7, 521–534, 2011

NA-GIN exchange impact deglacial AMOC

J. Cheng et al.

The reinitiation of deep-water formation in the GIN Sea is the combined results of the local and non-local factors during the recovery period of the AMOC. Based on above analysis, the local and non-local factors together induces the deep-water formation in the GIN Sea unrecovered, even a insignificant resumption (about 20% as to the DGL-A run) at the earlier part of the PB_REC run (Fig. 1). This feature is also confirmed by the convection (XMXL, Fig. 2e), which only resumes about 13% in the PB_PreBA run and about 38% in the PB_REC run. As restricted by the two factors, the convection and the deep-water formation can't resume further, and then no overshoot and the subsequent mean state transition of the AMOC be achieved.

The climatic impact of lack of the overshoot and mean state transition during the BA onset is shown with the SAT differences between the two sensitivity experiments and the DGL-A run at the time of 14.32 ka (maximum overshoot). SAT differences show negative values in the extratropical Northern Hemisphere and slightly positive values in the extratropical Southern Hemisphere for both sensitivity experiments (Fig. 3). The negative values in the extratropical Northern Hemisphere, with a maximum value of more than 15 °C over the GIN Sea points to a reduced SAT warming in the sensitivity experiments compared to the DGL-A run during the BA onset. Similarly, the positive values in the extratropical Southern Hemisphere indicate enhanced warming during the BA onset. This typical hemispheric "see-saw" pattern in the SAT mimics closely the climatic response to the AMOC strength change in other model studies (Stocker, 1998; Vellinga and Wood, 2002). The weaker SAT response in the PB_REC run is likely caused by the smaller reduction in the AMOC strength comparing to the PB_PreBA run (Fig. 3b). The analysis of a fresh water-hosing experiment under the Holocene conditions with CCSM3 indicate that the strength of the "see-saw" phenomenon depend on the magnitude of the AMOC strength change (not shown).

CPD
7, 521–534, 2011

4 Conclusions

Our sensitivity experiments with the CCSM3 explicitly demonstrate the impact of the oceanic NA - GIN Sea exchange, that it's critical for the achievement of the overshoot phenomenon and the subsequent mean state transition of the AMOC during the last deglaciation. The mechanism for the AMOC overshoot presented here advances and sheds further light on the mechanism shown in Liu et al., (2009). Furthermore, in comparison to other factors such as GHG, orbital insolation forcing and atmospheric processes, it is found that the internal oceanic exchange between the NA and GIN Sea is more important for the AMOC evolution during the BA onset.

The purpose of the implementation of PB scheme in the sensitivity experiments is to break the linkage between the NA and the GIN Sea. In other words, the effect of the PB scheme is to isolate the GIN Sea from the whole NA in terms of key oceanic processes. Based on our results we conclude that the participation of the GIN Sea in the recovery process of the AMOC is critical for the generation of the abrupt climate change during the glacial cycle. Other works also point out the fundamental importance of the GIN Sea to the deep-water formation in the Labrador Sea (Dickson et al., 2002) and to the changes of the AMOC strength under the possible climate change in the model simulations (Stouffer et al., 2006).

Our sensitivity experiments also point out that the recovery of deep-water formation in the Labrador and GIN Sea is not independent. In particular the model results show that, if the deep-water formation in the GIN Sea is kept in a suppressed state artificially, the change of the deep-water formation in the Labrador Sea will be affected too. This result confirms the conclusions from investigations of the temporal evolution of the deep-water formation during the Holocene period as inferred from the marine proxy records (de Vernal and Hillaire-Marcel, 2006; Hillaire-Marcel et al., 2007), and from an investigation of the AMOC response to anthropogenic forcing in a coupled model simulation (Hu et al., 2004).

CPD
7, 521–534, 2011

Supplementary material related to this article is available online at: http://www.clim-past-discuss.net/7/521/2011/cpd-7-521-2011-supplement.pdf.

Acknowledgements. This study is based on the model integrations preformed at NCAR, and the computation resources is provided by CCSM Paleoclimate Working Group. We thank Yafang Zhong for the contribution of PB scheme implementing. This work is supported by NSF, DOE, Peking University, Special public sector research of CMA, China (GYHY200906016) and NUIST (Y602).

References

Arzel, O., England, M. H., and Sijp, W. P.: Reduced stability of the Atlantic meridional overturning circulation due to wind stress feedback during glacial times, J. Clim., 21, 6260–6282, doi:10.1175/2008JCLI2291.1, 2008.

Barker S., Diz, P., Vautravers, M. J., Pike, J., Knorr, G., Hall, I. R., and Broecker, W. S.: Interhemispheric Atlantic seesaw response during the last deglaciation, Nature, 457(7233), 1097, doi:10.1038/nature07770, 2009.

Barker S., Knorr, G., Vautravers, M. J., Diz, P., and Skinner, L. C.: Extreme deepening of the Atlantic overturning circulation during deglaciation, Nat. Geosc., 3, 567–571, doi:10.1038/ngeo921, 2010.

Collins, W. D., Bitz, C. M., Blackmon, M. L., Bonan, G. B., Bretherton, C. S., Carton, J. A., Chang, P., Doney, S. C., Hack, J. J., Henderson, T. B., Kiehl, J. T., Large, W. G., McKenna, D. S., Santer, B. D., and Smith, R. D.: The Community Climate System Model Version 3 (CCSM3), J. Clim., 19, 2122–2143, doi:10.1175/JCLI3761.1, 2006.

Cuffey, K. M. and Clow, G. D.: Temperature, accumulation, and ice sheet elevation in central Greenland through the last deglacial transition, J. Geophys. Res., 102, 26383–26396, doi:10.1029/96JC03981, 1997.

de Vernal, A. and Hillaire-Marcel, C.: Provincialism in trends and high frequency changes in the northwest North Atlantic during the Holocene, Global Planet. Change, 54, 263–290, 2006.

Dickson, B., Yashayaev, I., Meincke, J., Turrell, B., Dye, S., and Holfort, J.: Rapid freshening of the deep North Atlantic Ocean over the past four decades, Nature, 416, 832–837, 2002.

Hillaire-Marcel, C., de Vernal, A., and Piper, D. J. W.: Lake Agassiz final drainage event in the northwest North Atlantic, Geophys. Res. Lett., 34, L15601, doi:10.1029/2007GL030396, 2007.

Hu, A., Meehl, G. A., Washington, W. M., and Dai, A.: Response of the Atlantic Thermohaline Circulation to increased atmospheric CO_2 in a coupled model, J. Clim. 17, 4267–4279, 2004.

Joos, F. and Spahni, R.: Rates of change in natural and anthropogenic radiative forcing over the past 20 000 years, P. Natl. Acad. Sci., 105, 1425–1430, doi:10.1073/pnas.0707386105, 2008.

Knutti, R., Fluckiger, J., Stocker, T. F., and Timmermann, A.: Strong hemispheric coupling of glacial climate through freshwater discharge and ocean circulation, Nature, 430, 851–856, doi:10.1038/nature02786, 2004.

Krebs, U. and Timmermann, A.: Tropical air-sea interactions accelerate the recovery of the Atlantic Meridional Overturning Circulation after a major shutdown, J. Clim., 20, 4940–4956, doi:10.1175/JCLI4296.1, 2007.

Liu, Z., Wu, L., Gallimore, R., and Jacob, R.: Search for the origins of Pacific decadal climate variability, Geophys. Res. Lett., 29(10), 1404, doi:10.1029/2001GL013735, 2002.

Liu, Z., Otto-Bliesner, B. L., He, F., Brady, E. C., Tomas, R., Clark, P. U., Carlson, A. E., Lynch-Stieglitz, J., Curry, W., Brook, E., Erickson, D., Jacob, R., Kutzbach, J., and Cheng, J.: Transient Simulation of Last Deglaciation with a New Mechanism for Bølling-Allerød Warming, Science, 325, 310–314, doi:10.1126/science.1171041, 2009.

Manabe, S. and Stouffer, R. J.: Coupled Ocean-Atmosphere Model Response to Freshwater Input: Comparison to Younger Dryas Event, Paleoceanography, 12(2), 321–336, doi:10.1029/96PA03932, 1997.

Mignot, J., Ganopolski, A., and Levermann, A.: Atlantic Subsurface Temperatures: Response to a Shutdown of the Overturning Circulation and Consequences for Its Recovery, J. Clim., 20(19), 4884–4898, doi:10.1175/JCLI4280.1, 2007.

Peltier, W. R.: Global Glacial Isostasy and the Surface of the Ice-Age Earth: The ICE-5G (VM2) Model and GRACE, Annual Review of Earth and Planetary Science, 32, 111–149, 2004.

Schmittner, A. and Galbraith, E. D.: Glacial greenhouse gas fluctuations controlled by ocean circulation changes, Nature, 456, 373–376, doi:10.1038/nature07531, 2008.

Stanford, J. D., Rohling, E. J., Hunter, S. E., Roberts, A. P., Rasmussen, S. O., Bard, E., McManus, J., and Fairbanks, R. G.: Timing of meltwater pulse 1a and climate responses to meltwater injections, Paleoceanography, 21, PA4103, doi:10.1029/2006PA001340, 2006.

CPD
7, 521–534, 2011

NA-GIN exchange impact deglacial AMOC

J. Cheng et al.

Stocker, T. F.: The seesaw effect, Science, 282, 61–62, 1998.
Stouffer, R. J., Yin, J., Gregory, J. M., Dixon, K. W., Spelman, M. J., Hurlin, W., Weaver, A. J., Eby, M., Flato, G. M., Hasumi, H., Hu, A., Jungclause, J., Kamenkovich, I. V., Levermann, A., Montoya, M., Murakami, S., Nawrath, S., Oka, A., Peltier, W. R., Robitaille, D. Y., Sokolov, A., Vettoretti, G., and Weber, N.: Investigating the causes of the response of the thermohaline circulation to past and future climate changes, J. Clim., 19, 1365–1387, doi:10.1175/JCLI3689.1, 2006.
Vellinga, M. and Wood, R. A.: Global climatic impacts of a collapse of the Atlantic thermohaline circulation, Climatic Change, 54, 251–267, 2002.
Weaver, A. J., Saenko, O. A., Clark, P. U., and Mitrovica, J. X.: Meltwater pulse 1A from Antarctica as a trigger of the Bolling-Allerod warm interval, Science, 299, 1709–1713, doi:10.1126/science.1081002, 2003.
Weber, S. L. and Drijfhout, S. S.: Stability of the Atlantic meridional Overturning Circulation in the Last Glacial maximum climate, Geophys. Res. Lett., 34, L22706, doi:10.1029/2007GL031437, 2007.
Wu, L. and Liu, Z.: Is Tropical Atlantic Variability driven by the North Atlantic Oscillation? Geophys. Res. Lett., 29(13), 1653, doi:10.1029/2002GL014939, 2002.
Wu, L., Liu, Z., Gallimore, R., Jacob, R., Lee, D., and Zhong, Y.: Pacific decadal variability: The tropical Pacific mode and the North Pacific mode, J. Clim., 16, 1101–1120, doi:10.1175/1520-0442(2003)16<1101:PDVTTP>2.0.CO;2, 2003.
Yeager, S. G., Shields, C. A., Large, W. G., and Hack, J. J.: The low resolution CCSM3, J. Clim., 19, 2545–2566, doi:10.1175/JCLI3744.1, 2006.
Zhong, Y., Liu, Z., and Jacob, R.: Origin of pacific multi-decadal variability in community climate system model, version 3 (CCSM3): A combined statistical and dynamical assessment, J. Clim., 21, 114–133, doi:10.1175/2007JCLI1730.1, 2008.

CPD
7, 521–534, 2011

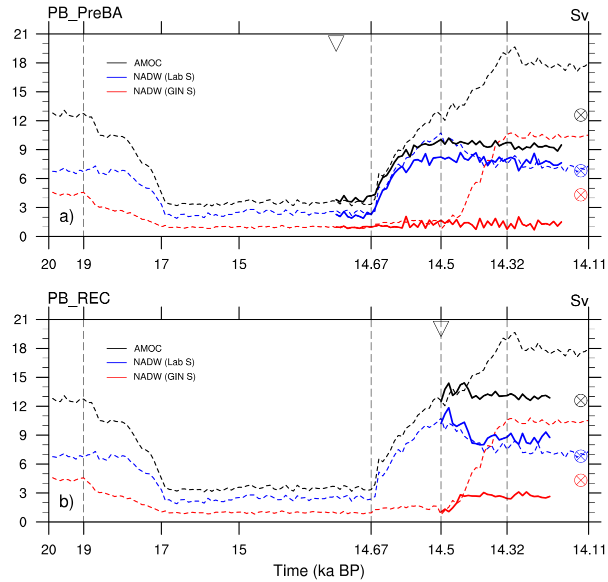

Fig. 1. AMOC strength (black solid line) and regional deep-water formation amount in the Labrador Sea (shown as "NADW (Lab S)", blue solid line) and the GIN Sea (shown as "NADW (GIN S)", red solid line) for the PB_PreBA **(a)** and the PB_REC **(b)** run. Dashed lines are the corresponding series in the DGL-A run. The AMOC strength is defined as the maximum streamfunction of NA under 500 m depth. The deep-water formation amount in the GIN Sea is defined as the vertical maximum value of streamfunction at the south edge of the GIN Sea (62° N). The deep-water formation amount in Labrador Sea is defined as the difference of the AMOC strength and the deep-water formation amount in the GIN Sea, assuming the AMOC strength defined here represents the total amount of the deep-water formation in NA. Inverted triangle and circles with colors of black, blue and red represent the restoring time of each sensitivity experiments, the LGM level of AMOC strength and regional deep-water formation amount in the Labrador and GIN Sea, respectively.

CPD
7, 521–534, 2011

NA-GIN exchange impact deglacial AMOC

J. Cheng et al.

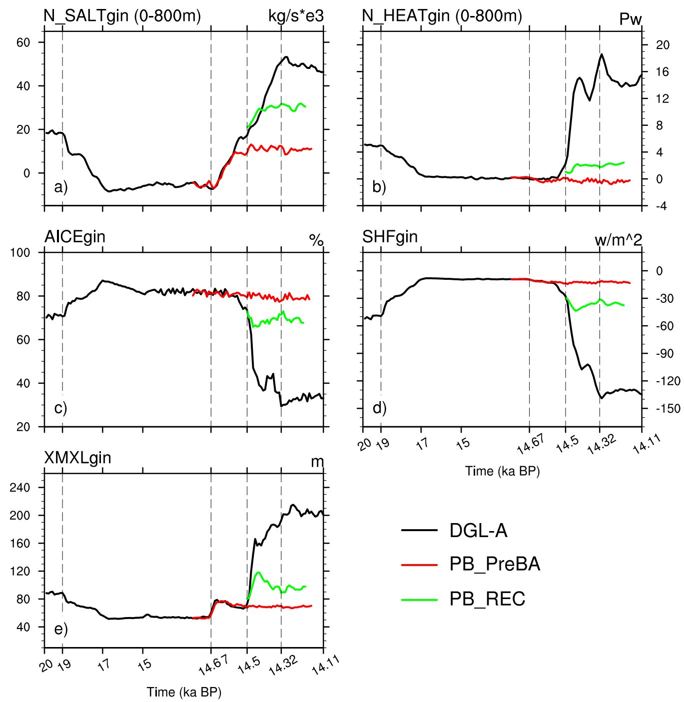

Fig. 2. Time series evolution of upper layer (0–800 m) salt **(a)** and heat **(b)** transport to the GIN Sea, sea ice concentration (AICE, **(c)**), surface heat flux (SHF, **(d)**) and maximum mixed layer depth (XMXL, **(e)**) area means in the GIN Sea. Variables in the DGL-A, the PB_PreBA and the PB_REC runs are shown with colors of black, red and green, respectively. All plots are based on the decadal mean data.

CPD
7, 521–534, 2011

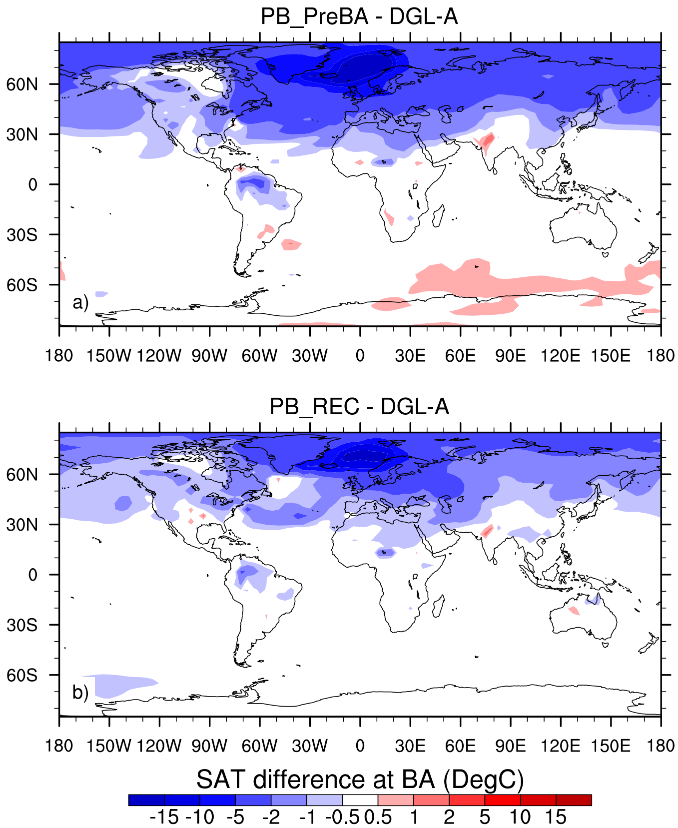

Fig. 3. SAT difference of the PB_PreBA **(a)** and the PB_REC run **(b)** to the DGL-A run at the time of 14.32 ka (maximum AMOC overshoot, seen in Fig. 1).

CPD
7, 521–534, 2011

NA-GIN exchange impact deglacial AMOC

J. Cheng et al.